This article was downloaded by:
On: *22 January 2011*
Access details: *Access Details: Free Access*
Publisher *Taylor & Francis*
Informa Ltd Registered in England and Wales Registered Number: 1072954 Registered office: Mortimer House, 37-41 Mortimer Street, London W1T 3JH, UK

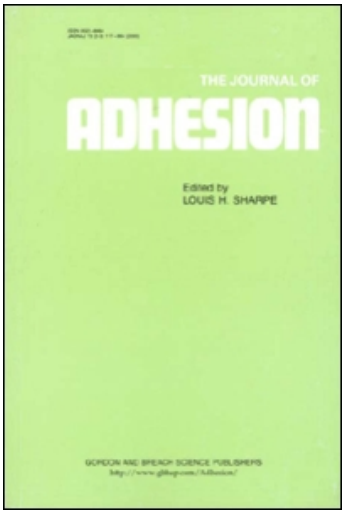

The Journal of Adhesion
Publication details, including instructions for authors and subscription information:
http://www.informaworld.com/smpp/title~content=t713453635

Use of an Optical-Mechanical Test Combined with Acoustic-Emission Techniques to Study Adhesion in Filled Polymeric Composites

Felix N. Nguyen[a]; John C. Berg[a]
[a] Department of Chemical Engineering, University of Washington, Seattle, Washington, USA

To cite this Article Nguyen, Felix N. and Berg, John C.(2005) 'Use of an Optical-Mechanical Test Combined with Acoustic-Emission Techniques to Study Adhesion in Filled Polymeric Composites', The Journal of Adhesion, 81: 7, 823 — 841
To link to this Article: DOI: 10.1080/00218460500189166
URL: http://dx.doi.org/10.1080/00218460500189166

PLEASE SCROLL DOWN FOR ARTICLE

Full terms and conditions of use: http://www.informaworld.com/terms-and-conditions-of-access.pdf

This article may be used for research, teaching and private study purposes. Any substantial or systematic reproduction, re-distribution, re-selling, loan or sub-licensing, systematic supply or distribution in any form to anyone is expressly forbidden.

The publisher does not give any warranty express or implied or make any representation that the contents will be complete or accurate or up to date. The accuracy of any instructions, formulae and drug doses should be independently verified with primary sources. The publisher shall not be liable for any loss, actions, claims, proceedings, demand or costs or damages whatsoever or howsoever caused arising directly or indirectly in connection with or arising out of the use of this material.

The Journal of Adhesion, 81:823–841, 2005
Copyright © Taylor & Francis Inc.
ISSN: 0021-8464 print/1545-5823 online
DOI: 10.1080/00218460500189166

Taylor & Francis
Taylor & Francis Group

Use of an Optical–Mechanical Test Combined with Acoustic-Emission Techniques to Study Adhesion in Filled Polymeric Composites

Felix N. Nguyen
John C. Berg
Department of Chemical Engineering, University of Washington, Seattle, Washington, USA

The use of acoustic-emission (AE) techniques integrated with single-particle composite (SPC) mechanical–optical testing is proposed to evaluate and characterize adhesion in particle-filled polymeric composites. It is shown that not only can an intrinsic interfacial strength be determined but also that different types of adhesion mechanisms may be distinguished in terms of straightforward criteria using the wavelet transform (WT) of the acoustic signature, once problems with internal reflections in the test coupon are resolved. The validity of the proposed method is demonstrated with a study of the adhesion of a commercial poly(vinyl-butyral) (PVB) to bare and aminosilane-treated glass beads.

Downloaded At: 08:44 22 January 2011

Keywords: Acoustic emission (AE); Adhesion; Glass beads; Particle-filled composites; Poly(vinyl butyral) (PVB); Single-fiber fragmentation composite (SFC) test; Single-particle composite (SPC) test; Wavelet coefficient (WC) ratio; Wavelet transformation (WT)

1. INTRODUCTION

When a particle-filled or fiber-reinforced composite material is strained sufficiently it will fail by one or a combination of events, including delamination at the phase boundaries or crack or craze formation and growth in the matrix or in the filler particles or the reinforcing fibers. For idealized situations involving transparent matrix

Received 21 January 2005; in final form 20 April 2005.
One of a collection of papers honoring Manoj K. Chaudhury, the February 2005 recipient of The Adhesion Society Award for Excellence in Adhesion Science, sponsored by 3M.
Address correspondence to John C. Berg, Department of Chemical Engineering, University of Washington, Box 351750, Seattle, WA 98195-1750, USA. E-mail: berg@cheme.washington.edu

materials, mechanical–optical tests have been devised to determine the conditions leading to delamination, *i.e.*, adhesive failure. For systems of simple geometry and known bulk mechanical properties, elasticity theory may be applied to determine the local stress concentration at the interface. Fracture-mechanics theory may then be used to infer the interfacial strength from the measured applied stress at failure. For example, the single-fiber fragmentation composite test (SFC) [1, 2] has been widely used to estimate the strength of the fiber–matrix interface. A coupon containing a single fiber is subjected to an increasing tensile load in the direction of the fiber axis until the fiber fractures into fragments whose ultimate size distribution can be related approximately to the interfacial strength. More recently, the single-particle composite (SPC) test [3–5] has been used for determining the strength of the interface between a spherical inclusion and its effectively infinite surrounding matrix. In this test, a coupon containing a single particle is strained until a delamination cap is observed at one of the particle poles. An analytical solution, available for this geometry, relates the measured applied stress at the moment of delamination to the stress at the pole and to the work of adhesion [4, 5]. In both of these tests, under some circumstances, bulk matrix cracking or crazing may be observed in addition to interfacial delamination, and their presence, sometimes detectable only by postmortem examination of the failed specimen, may render difficult or even impossible the inference of interfacial strengths.

Downloaded At: 08:44 22 January 2011

Mechanical–optical tests of this type are not amenable for use with opaque specimens nor do they provide information concerning events of small enough geometric inclusions that they avoid optical detection. An alternative approach that may overcome such limitations is that of detecting and characterizing the acoustic emission (AE) that accompanies any of the previously mentioned events. After first being applied by Kaiser in 1953 [6], AE has developed rapidly as a nondestructive test for investigating the behavior of materials deforming under stress. Microscopic events in the material give rise to elastic sound waves that propagate outward from the location of the event and are detectable using one or more piezoelectric transducers affixed to the surface of the specimen. The signal from the event, which is amplified and recorded, provides a record of the event's occurrence and its location in the specimen, and such information has been the principal objective of AE testing. Using an AE system, small-scale damage may be detectable long before critical failure. Beyond this, however, the acoustic signature, properly analyzed, contains information that may be used to distinguish between the many modes of active damage in

the stressed material, such as filler or reinforcement debonding, growing cracks or crazes, fiber breakage, and so forth.

The quantitative analysis of AE signals obtained during the testing of a specimen is complex and fraught with potential ambiguities, as described in detail throughout the article. The simultaneous acquisition of optical and acoustic records, however, holds the promise of identifying certain features of the acoustic signature with certain types of events, as observed directly. Indeed, this approach was used recently in the authors' study of the effect of vinyl alcohol (OH) content on the adhesion of poly(vinyl butyral) (PVB) to embedded glass spheres [5]. The adhesion of PVB to glass is crucial to the production of shatter-resistant, or *enhanced protective*, glass (EPG). Not only did the acoustic signals correlate exactly with the observed debonding events, but they were also capable of distinguishing weak from strong adhesion. In the former case (low OH content), a single high-amplitude acoustic hit was obtained, indicating an instantaneous detachment of the entire cap, whereas, for strong adhesion (high OH content), a series of low-to-intermediate-amplitude hits (separated by a few microseconds) suggested a stepwise detachment. It was also possible to separate interfacial debonding from other events in terms of the times at which they occurred.

In the present work, we desire to investigate further the simultaneous use of mechanical–optical tests and AE analysis to formulate straightforward criteria to distinguish different types or levels of adhesive bonding from one another and to address some of the ambiguities inherent in AE testing of composite materials. The study is performed using single glass spheres, either untreated or treated with various aminosilanes, embedded in a PVB matrix.

Downloaded At: 08:44 22 January 2011

2. MATERIALS AND METHODS

2.1. Materials and Testing

PVB (Mowital B60HH, 12% hydroxyl content) was provided by Kukaray America Inc. (New York, NY, USA). Soda-lime glass beads of 900 μm in diameter (Grade A090) provided by Potters Industries, Inc. (Valley Forge, PA, USA) are cleaned with Nochromix, from Godax Labs., Cabin John, MD, USA, then treated with three silanes obtained from Gelest Inc. (Morrisville, PA, USA): 3-aminopropyltrimethoxy silane (APS), N-(6-aminohexyl)aminopropyltrimethoxy silane (AH-APS), and (3-trimethoxysilylpropyl)diethylenetriamine (DAE-APS). The procedure for the treatment was recommended by Harding and Berg [7] for complete coverage. The composition of these silanes in

deionized water in each case was 0.5 vol.% to inhibit the interaction of the amino group with a hydroxyl group of either the silane itself or of the substrate [8].

Using a procedure identical to that described in our previous study [5], smooth-edged specimens (30 mm × 110 mm × 3 mm) of PVB, each containing a single glass bead in PVB sample, were prepared and uniaxially strained in a Satec T-1000 mechanical tester (Satec Systems, Inc., Grove City, PA, USA) until a debonding event appeared at one of the poles of the particle, accompanied by AE hits. The transducers used for acquisition of the acoustic data were two wide-band and flat-band HD2WD purchased from Physical Acoustics Corporation (Princeton Junction, NJ, USA). Each is mounted 10 mm from the bead, and 20 mm from the tip of the grip. For each run, optical and AE data were collected for further analysis. At least five specimens were tested for each type of treatment. Wavelet transformation (WT), as discussed later, was performed on the AE data using free software, *viz*. Vallen Wavelet from Vallen Systems (Munich, Germany, http://www.vallen.de).

Downloaded At: 08:44 22 January 2011

2.2. AE Propagation in Thin Plates and AE Analysis

2.2.1. Sound-Wave Propagation in Bounded Elastic Solids

Because AE signals are sound waves in confined media, it is necessary first to consider their general nature. Bulk sound waves, once released by a failure event in a bounded medium, propagate in the medium in a complicated way. Such complications render difficulties to their analysis in practice. There are two types of bulk waves accompanying the failure: *longitudinal* (pressure) *P waves* and *transverse* (shear) *S waves* propagate in the medium such that they induce the medium elements' motion parallel or perpendicular to the wave-propagation direction, respectively. S waves propagate with slower velocity and can be classified into *vertically polarized* (SV) and *horizontally polarized* (SH) *waves* based on the elements' motion confined in the plane of the wave propagation or out of the plane, respectively. It is found that when a wave of either longitudinal or transverse type impinges obliquely on an interface between two media, both reflection and refraction take place. Although an incident SH wave generates only a refracted and a reflected SH wave, similar to light, an incident P wave or SV wave produces not only refracted and reflected P waves but also refracted and reflected SV waves (Figure 1). The mode conversion is due to the mixed boundary conditions of continuity on the stresses and the displacements at the interface of the two half-spaces [9].

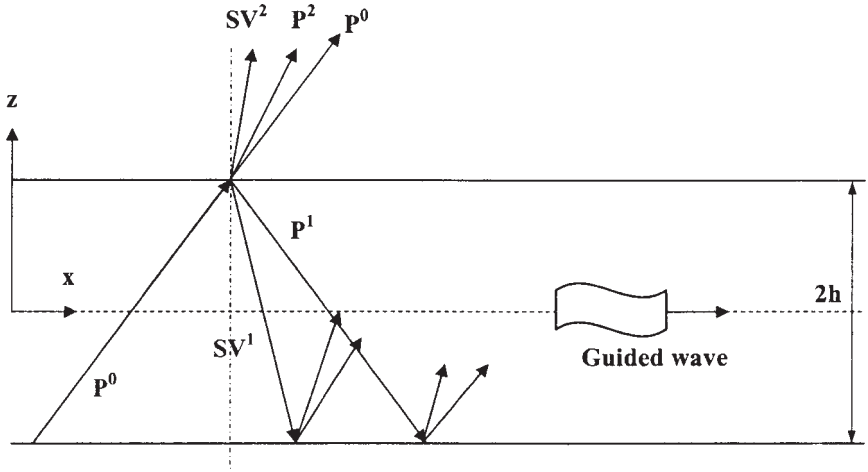

FIGURE 1 Waveguide in an elastic plate. For a wave plane in a plate, only incident P and SV waves are considered, and the particle motions are constrained in the x-z plane with uniform physical properties in the y direction. An incident P wave (P^0) will generate a reflected (P^1) and a refracted (P^2) P wave as well as a reflected (SV^1) and a refracted (SV^2) SV wave. Similarly, an incident SV wave will generate four waves. The guided wave in the plate will propagate in the x direction. Spatial elements will move bidirectionally at a distance of a few multiples of the plate thickness, and their motions can be split into symmetric and antisymmetric Lamb waves.

Downloaded At: 08:44 22 January 2011

The condition for this conversion depends on the incident angle and the medium's properties.

Increased complexity of wave propagation arises when the medium is a layer bounded by two interfaces (*e.g.*, a plate with infinite lateral dimensions). A wave can propagate in the layer by being reflected back and forth between the two plane surfaces and convert back and forth between P and SV waves (Figure 1). This gives rise to *dispersion*, *i.e.*, the wave changes velocity with respect to both frequency and wavelength as it passes through the layer. The *group velocity* is usually used to describe this wave propagation in terms of its energy. Dispersion governs the shape of a pulse as it propagates through a medium. Such a system is termed a *waveguide*, and a resultant wave, formed in the waveguide by superposition of a system of incident and reflected waves, is called a *guided wave*. The movements of medium elements as the guided wave propagates are quite complex; however, they can be split into *longitudinal* (symmetric) and *transverse* (antisymmetric) *Lamb waves* [9]. These Lamb waves can propagate in the plate

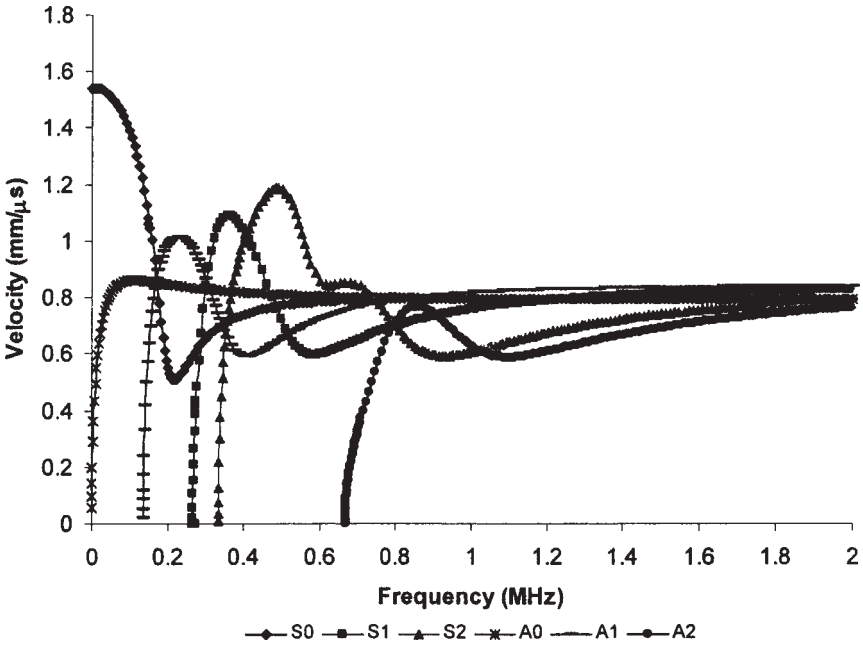

FIGURE 2 Possible dispersion group velocity curves of a PVB plate of 3.1-mm thickness and infinite lateral dimensions whose Young's modulus is 2.2 GPa, density 1100 kg/m^3, and Poission's ratio 0.4. The resulting bulk velocities are $c_1 = 2.0170$ m/s and $c_2 = 0.8452$ m/s. This shows how complicated the wave propagation in a plate is, as demonstrated by the symmetric (S_0, S_1, etc.) and antisymmetric (A_0, A_1, etc.) velocity curves.

Downloaded At: 08:44 22 January 2011

independent of one another, each with a unique velocity. The number of longitudinal or transverse modes present in the guided wave depends on the thickness of the cross section. An example of all possible Lamb modes identified by corresponding dispersion curves in a PVB plate 3.1 mm thick is shown in Figure 2.

Additional complications arise when the medium has finite *lateral* dimensions. Imagine that SH waves possibly emitted from a source and P and SV waves reflected from edges might be superimposed on the guided wave, resulting in a very complex wave. This complexity is not desired for practical applications, in which source identification and its location are sought.

2.2.2. Acoustic-Emission Propagation in a Thin Plate

Acoustic emission is defined as the transient wave emission caused by a spontaneous release of energy when materials deform or fracture

when subjected to load. If the stress field is elastic, a guided wave is formed as a result of interactions of a number of bulk longitudinal and transverse waves emitted by the source. A snapshot of this wave, called a *hit*, is captured by a sensor mounted on a surface of the plate. Such a guided wave almost always produces dispersion [10]. The frequency content of the waveguide (which identifies the constituents of the source) does not change with propagation distance provided only negligible absorption occurs. However, the signal length broadens at longer propagation distances because of the dispersion.

A misconception in AE analysis is that the nature of the source alone controls the measured frequencies. This is true only when the bulk waves are measured directly. The actual frequencies that are recorded with a perfectly flat-frequency-band, surface-mounted sensor on a plate are determined by energetic portions of the Lamb modes in the plate that are excited by the source (*i.e.*, no reflections whatsoever). Key factors are the thickness of the plate and the depth of the source in the plate and the material's properties (*e.g.*, density, Young's modulus). For many AE studies, the test specimens are usually small, thin plates. As a result, a guided wave with both longitudinal (S_0) and transverse (A_0) Lamb modes, which have both in-plane and out-of-plane components, is commonly observed. In AE measurements, it is usually the out-of-plane component that is measured, because the measurement is made on the surface of the plate rather than the edge. Edge reflections, because of smallness of coupons, interfere with the direct source-to-sensor signals and often make the measurements potentially erroneous [10, 11].

Downloaded At: 08:44 22 January 2011

2.2.3. AE-Analysis Approaches

The common approach for AE analysis is to use direct data, such as amplitude, duration, rise time, counts, and energy, and to correlate their magnitudes to various expected modes of failure in a composite [12–16]. Recently, in adhesion studies, AE signals and/or their amplitudes have been used not only to detect failure events in filled polymeric specimens but also to quantify adhesion strength, which is correlated to the maximum of a fitted Weibull distribution of the events [17–24]. Nevertheless, this approach is often found to be ambiguous and necessitates definition of a combined analysis of several direct AE parameters to be correlated unique type of physical damage [25]. Two reasons for this ambiguity are (1) the lack of direct confirmation of the source mechanisms to compare with the AE data, and (2) complexities associated with the use of small laboratory coupons without confirmation of the effect of nearby edge reflections on the AE parameters. Therefore, the source mechanisms are usually just assumed

without justification, based on the types of damage expected in the given laminate structure or from post-mortem examination of the fractures. Simultaneous acquisition of optical records and AE specific characteristic signatures should allow delineation of these mechanisms.

A better approach is to analyze the general form of the acoustic wave produced from a source. Spectral analysis such as the Fast Fourier Transform (FFT) is the standard tool by which a signal is decomposed into basic sine and cosine functions. The result is an averaged frequency spectrum of the signal. Nevertheless, this technique is not appropriate for burst-type signals such as AE signals, which require a more time-revealing tool. Such a tool is the WT [26]. Wavelet analysis involves a fundamentally different approach. Instead of breaking down a wave function into harmonic functions, like FFT, the signal is broken into a series of functions of short duration called *wavelets*. Commonly, each wavelet is a product of a continuous wave of either sine or cosine function and a *window function* of Gaussian form whose band width and amplitude are both scaled with respect to frequency. This window is shifted along the signal by sampling a time length (Δt) and, for every position of the window, the spectrum (by FFT) is calculated. The process is repeated as many times as desired, each time with a slightly narrower or broader window. This variable window-length characteristic of the wavelet is obviously suited for the analysis of AE signals whose high-frequency components are analyzed with short-time, wide-frequency windows, and low-frequency components with extended-time, low-frequency windows.

The result of WT of a source signal is a collection of *wavelet coefficients* (WCs) or wavelet amplitudes, which have units of power (mV or dB) and depend on both time and frequency. These coefficients relate the wavelets to the original waveform such that the higher the relative magnitude of the coefficient at a given time, the greater the chance that the original waveform contains a particular wavelet

FIGURE 3 A typical WT spectrogram of an edge pencil break reproduced by Matlab (The Mathworks, Natick, MA, USA) in grayscale. The spectrogram is a two-dimensional contour map in time and frequency with the brightness representing the WCs or respective intensities of the transform at points in the time–frequency plane (a). The contour profile is basically the same as the fingerprint, and shows how the signal intensity of a particular frequency changes with time (microsecond, μs). The local maximum wavelet coefficient (with respect to time) at 500 kHz (WC_{max}); the average wavelet coefficients (WC_{avg}) over time at that frequency are shown in (b), for an example. For this source, there are two peaks on the map at 100 and 500 kHz, which are the characteristic peaks of these ABS plates.

Downloaded At: 08:44 22 January 2011

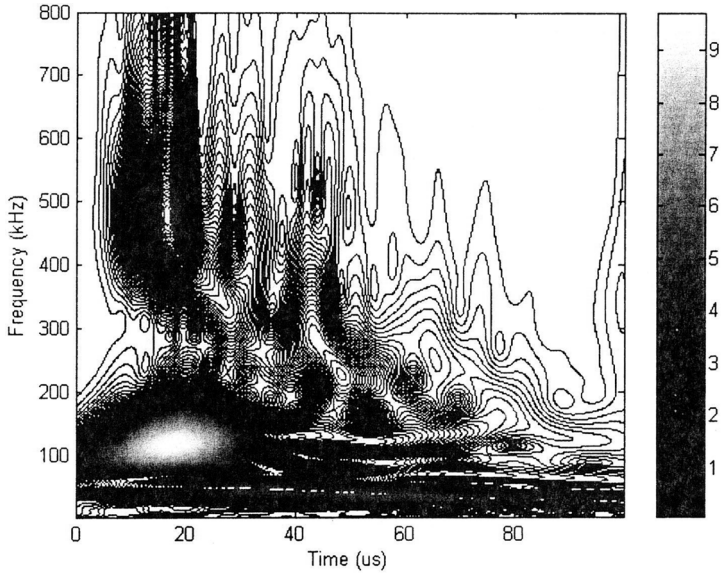

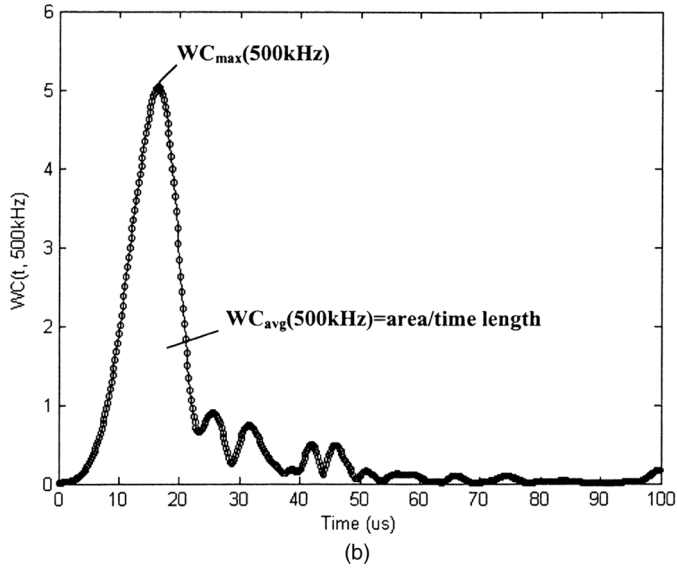

as identified by its center frequency and the amplitude of its FFT. This information is presented in a two-dimensional spectrogram or contour map of amplitudes (WCs) as a function of time and frequency, as shown in Figure 3a, for example. The contour profile is basically a

Downloaded At: 08:44 22 January 2011

fingerprint and shows how the signal intensity of a particular frequency changes with time. The local maximum WC (with respect to time) for each frequency (WC_{max}) in Figure 3b tells at what instant in the analyzed time length a wavelet is most likely to resemble the original waveform, whereas the average wavelet coefficient (WC_{avg}) over time tells how the energy of the original signal is distributed over that period of time at the frequency. Found on the spectrogram, usually, are areas of relatively high WC_{max} (bright areas against darker background), centered by a particular frequency and time, called *frequency range peaks* (or patterns). These peaks represent particular Lamb modes in the plate excited by the source. They usually are broad both in time and frequency, and their intensities show levels of excitement. As a result, the highest WC and the highest average WC of a peak of a source are usually observed at locations different from each other and from those of another source. Consequently, frequency-range patterns are found to be unique characteristics of a waveform and could be used as a basis of identify AE sources by type. For example, Suzuki *et al*. [26] have claimed that fiber fracture, matrix crack, and debonding failures produced in a glass-fiber-reinforced polymer composite under tensile load could be distinguished in terms of such pattern recognition. However, in a computational study, Hamstad *et al*. [27] have demonstrated that such pattern recognition is not sufficient to distinguish their three different simulated sources, namely, in-plane dipole, out-of-plane dipole, and crack initiation, in an aluminum plate with large lateral dimensions. They showed that these sources have qualitatively similar patterns (or shapes) to one another and do not depend on the distance between the source and the sensor but rather the distance from the source to the top surface where a sensor is mounted. The peak intensity was also shown to be significantly different from case to case. It was then suggested that the overall pattern seen in the WT spectrogram might be more characteristic of the plate medium than of the source, given no complications in the medium (*i.e*., no edge reflections), because sound from different sources propagates with similar group velocities in a given plate. This is the most common misconception of many AE practitioners. Consequently, Hamstad *et al*. [27] proposed the use of WC ratios of two fixed frequencies for the identification and showed that these WC ratios are significantly different among the three sources.

2.2.4. Method for Determination of Laboratory Coupon Size

Because there are difficulties with the AE analysis arising from small coupons that could affect the interpretation of information

Downloaded At: 08:44 22 January 2011

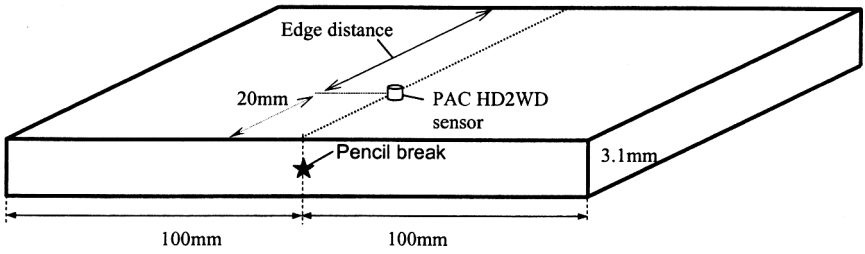

FIGURE 4 Experimental setup to determine the effect of edge reflections. The acrylonitrile-butadiene-styrene (ABS) plate is analogous to a PVB plate of similar thickness. The source is lead pencil breaks at an edge of the plate.

obtained by the WT technique, the effect of edge reflections on features of a WT spectrogram should be documented, and the appropriate coupon size selected for the adhesion study. As discussed previously, WC ratios would be better descriptors quantitatively representing a source. The constraints for the WC ratio comparison to be meaningful are that not only all the interrogated sources propagate in a plate with similar mechanical properties and thickness, but also that they are all released at a similar depth from the top surface, where a sensor is mounted.

The edge-pencil-break source used to investigate the effect of edge reflections in the ABS plate is analogous to an imbedded source in a PVB plate of similar thickness, because Young's modulus, density, and thickness are effectively the same. Hence, edge pencil breaks from Pentel 2 H leads (Pentel, Torrance, CA, USA) on three ABS plates, 3.1 mm thick and 200 mm long were used as a fixed source, and the edge-reflection effect was monitored with various sample widths. These breaks were performed exactly every time at the midplane of an edge of each plate. Each sample width is represented by an edge distance defined as the distance from the sensor, located along the centerline of the coupon, to the far edge. For this investigation, the three edge distances are 8, 15, and 57 mm. The distance from the source to the sensor was kept at 20 mm. The schematic is shown in Figure 4.

2.2.5. Method for Determination of Unique Descriptors for an Interrogated Source in a Thin Plate

As discussed, the only difference in WT spectrograms among interrogated sources in a given plate is essentially the differences in WCs of the peaks given no edge reflections and all sources released at a similar depth. Therefore, WC ratios of two fixed frequencies, *i.e.*, WC_{max}

Downloaded At: 08:44 22 January 2011

$(f_1, t_1)/WC_{max}$ (f_2, t_2) and WC_{avg} $(f_1, \Delta t)/WC_{avg}$ $(f_2, \Delta t)$, would best be used to capture the relative WC changes among the sources over a fixed time interval Δt (of 50 μs). For practical purposes, the selection of these frequencies is determined from examination of the WT spectrograms of the different source types identified optically with the SPC technique such that these two frequencies each correspond to a region of high WC_{max}. This method is simpler than that proposed by Hamstad *et al*. [27] who required Lamb mode identification and group velocity comparison.

3. RESULTS AND DISCUSSION

3.1. Minimum Coupon Size Determined by WC Ratios

Figure 3 shows a typical WT spectrogram of an edge pencil break. Two peaks (bright areas) centered at 100 kHz (very intense) and 500 kHz (much less intense) are the characteristic peaks of the ABS plates. After examining all spectrograms from various edge distances, the frequencies of 102 and 500 kHz were selected to represent these Lamb modes in the plates. The selection was verified by the reproducibility of their corresponding WC ratios over a succession of pencil breaks. For each edge distance the reproducibility was determined to be greater than 95%. These results imply that these ratios provide the characteristic signature of the edge-pencil-break source, and the comparison of these ratios at different edge distances can be used to determine the minimum sample width to avoid the effect of edge reflections on the collected signals. The comparison in Figure 5 shows that the variation of the WC_{max} and WC_{avg} ratios are less than 7%, respectively, when going from 15 to 57 mm. This finding suggests that the minimal edge distance, measured from the sensor to the far edge, is approximately 15 mm, which implies a minimum coupon width of 30 mm.

3.2. Distinguishing Adhesion Mechanisms using WC Ratios

It has been shown in the authors' early study of glass/PVB systems [5] that two debonding mechanisms are observed. The single debonding event observed in the case of an untreated glass bead in low OH-content PVB is thought to occur as the stress eventually grows large enough to suddenly detach the particle from the matrix, resulting in a single high-amplitude AE (a single hit). In contrast, in cases of aminosilane-treated glass beads in low OH-content PVB and bare glass beads in high OH-content PVB, a gradual increase in stress causes the particle to detach from the matrix in multiple steps over a few

Downloaded At: 08:44 22 January 2011

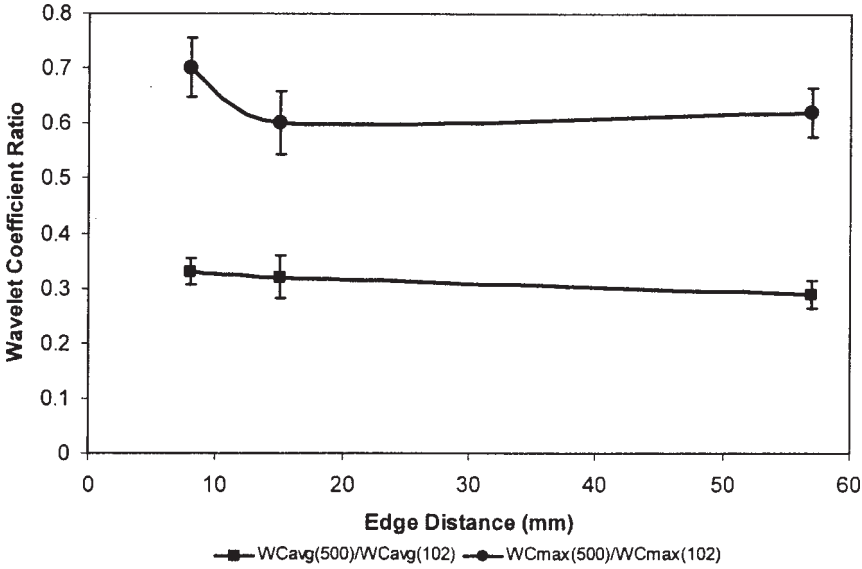

FIGURE 5 WC ratios at various edge distances. Two fixed frequencies of 102 and 500 kHz, each from an area of high WC_{max}, were selected, and their local maximum and average WCs greater than 50 μs were ratioed and used for the comparison. As shown, the variations in these ratios are less than 7% from 15 to 57 mm. This finding suggests that the minimal edge distance is 15 mm or the sample width is approximately 30 mm (twice as much as the edge distance).

Downloaded At: 08:44 22 January 2011

milliseconds, resulting in multiple AEs. These observations suggest that the single event debonding is associated with weaker adhesion, whereas stepwise debonding occurs when adhesion is stronger.

The stronger adhesion encountered may be of two mechanistic types, however. For the case of untreated glass beads, the *interface* is considered abrupt, so that strong *contact adhesion* develops as the number of hydroxyl groups in the polymer is increased, escalating the areal density of covalent bonds formed from the condensation of such groups with hydroxyl groups on the glass surface. Strong adhesion may also develop in the case of silane-treated glass surfaces when the organofunctional groups of the silane are of sufficient size and compatibility to penetrate the polymer, producing an *interphase* [28]. An example of this adhesion promotion *via* such a *diffusion* mechanism is the case of aminosilane-treated glass bead/PVB. The degree of adhesion strength is found to be dependent on both the number of the amino groups and their lengths in the present study. The adhesion

strength quantified from the applied stress at which the debonding initiates, *i.e.*, *failure stress*, is shown in Figure 6 for various glass bead/PVB systems. As shown, a higher stress (32 MPa) is required to detach a triaminosilane-treated glass bead from the matrix compared with a monaminosilane (APS)-treated bead (24.5 MPa) and an untreated bead (15 MPa). However, a similar stress is required to debond a glass bead treated with AH-APS whose length is comparable with that with DEA-APS. This result was also found in the previous studies [3, 4] in which a similar stress was required to debond a glass treated with APS or n-aminoethylaminopropyltrimethoxysilane (AE-APS), whose length is again comparable with that of APS.

Clearly, a measurement of adhesion strength correlates well to a degree of adhesion promotion. Nevertheless, it cannot distinguish

Downloaded At: 08:44 22 January 2011

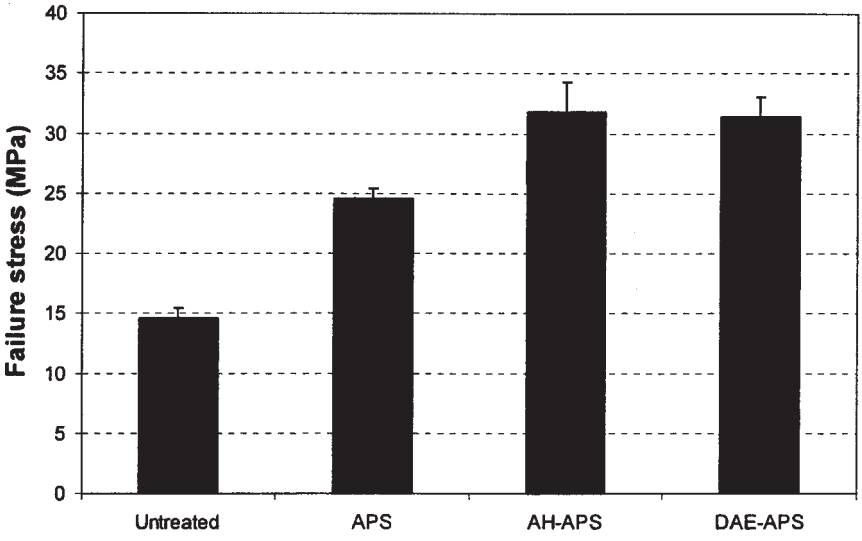

FIGURE 6 Comparison of failure stress of glass beads treated with various aminosilanes from PVB. Aminosilane-treated glass beads show a higher stress than the untreated. Glass beads treated with diaminosilane (AH-APS) and triaminosilane (DAE-APS) require a higher stress than glass beads treated with monoaminosilane (APS). Both the organofunctional group's length and the compatibility of the organofunctional groups with the hydroxyl groups of PVB play a role in the adhesion promotion; however, these factors cannot be separated. This adhesion promotion is *via* a *diffusion adhesion mechanism*, whereas in the untreated case it is *via* a *contact adhesion mechanism* because the interactions happen essentially at the interface between the glass surface and the polymer.

from which mechanism this degree of adhesion promotion is amplified. In other words, strong adhesion originating from a strong contact mechanism and a diffusion mechanism of a certain level of penetration would yield the same adhesion strength. This is seen in the cases of untreated glass/intermediate OH-content PVB (B60H) in the previous study [5] and of triamiosilane-treated glass bead/low OH-content PVB (B60HH) in the present study, both of which give a failure stress of about 32 MPa. Distinction among different adhesion mechanisms is often of interest when theoretical predictions are sought (for screening purposes), because each mechanism has its own criteria or a set of parameters required for the calculations. For that purpose, our hope is that examining the hidden information contained in the debonding AE waves resulting from various levels of adhesion using the WT may reveal some useful descriptor that allows us to distinguish between contact and diffusion adhesion mechanisms as well as the level of penetration. Only bare and aminosilane-treated glass beads in low OH-content PVB are considered for the investigation.

Downloaded At: 08:44 22 January 2011

Following the same procedure as in the edge reflection study, frequencies of 140 kHz and 500 kHz were selected for the formation of WC ratios after examining WT spectrograms of various sample types. Figure 7 shows WT spectrograms of a typical diffusion adhesion hit in a series and a typical contact adhesion hit. It is noticed that all aminosilanes share similar spectrograms on which there are always two distinguishable peaks centered at about 150 kHz and 520 kHz. The first hit of such a debonding event is thought to contain the most useful information and, therefore, is used for further analysis. As for contact adhesion, the peak centered at 140 kHz is very intense and reproducible up to 95%. The peak centered at about 500 kHz is usually recognizable. Because both frequencies of 140 and 500 kHz are also contained in the peaks in the former case, it is thought that they could meaningfully represent Lamb modes in the PVB plates. Consequently, their WC ratios were used to compare contact adhesion against diffusion adhesion mechanisms.

Figure 8 shows a comparison of WC ratios among different studied cases. As seen, the APS-treated glass bead shares similar WC ratios with the untreated bead, and its absolute maximum WC is found to have occurred at about 140 kHz as seen in the case of the untreated glass bead. An explanation for this is that the aminopropyl group of APS is short and would not penetrate to a great extent to the PVB polymer, which suggests a strong contact-adhesion mechanism.

The increase in WC ratios when going from monoamino- to diamino- to triamino-silane reveals the clear distinction between the contact

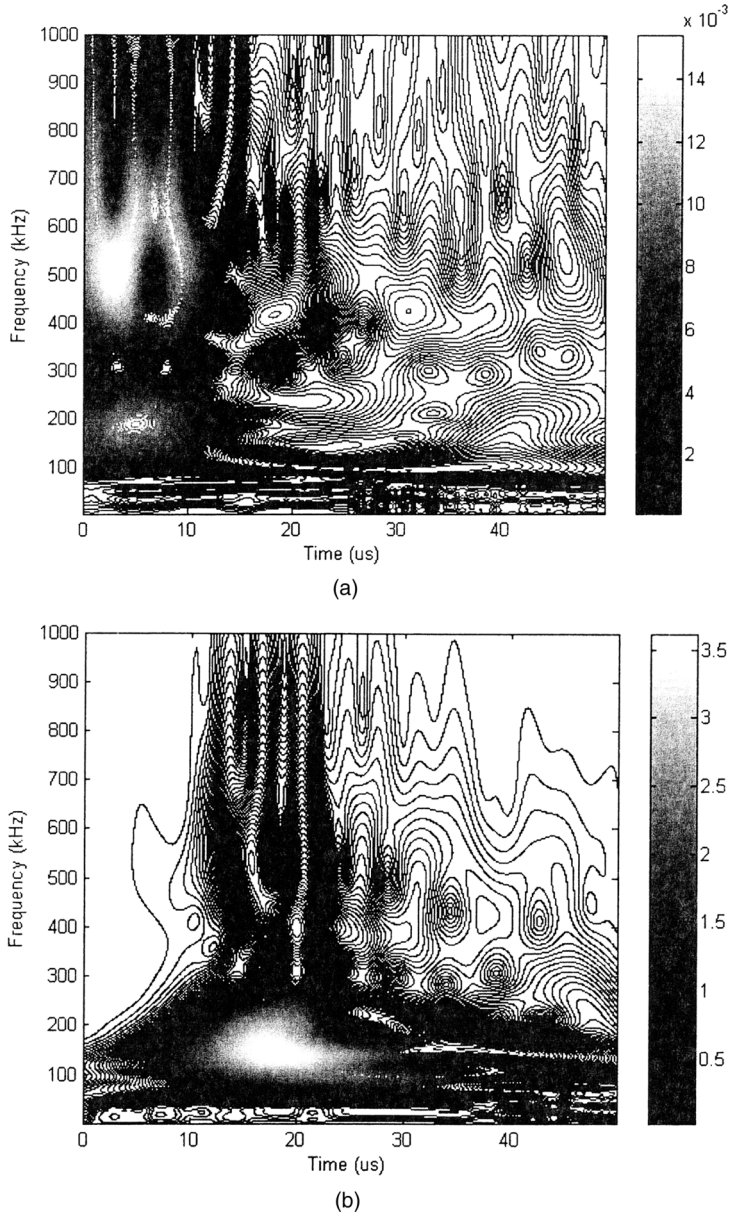

FIGURE 7 WT spectrograms of a typical diffusion adhesion hit in a series (triaminosilane-treated glass bead) and a typical contact adhesion hit (bare glass bead) reproduced by Matlab. It is noticed that all aminosilanes share similar spectrograms (a) in which there are always two distinguishable peaks centered at about 150 kHz and 520 kHz. As for contact adhesion (b), the peak centered at 140 kHz is very intense and reproducible up to 95%. The peak centered at about 500 kHz is usually recognizable.

Downloaded At: 08:44 22 January 2011

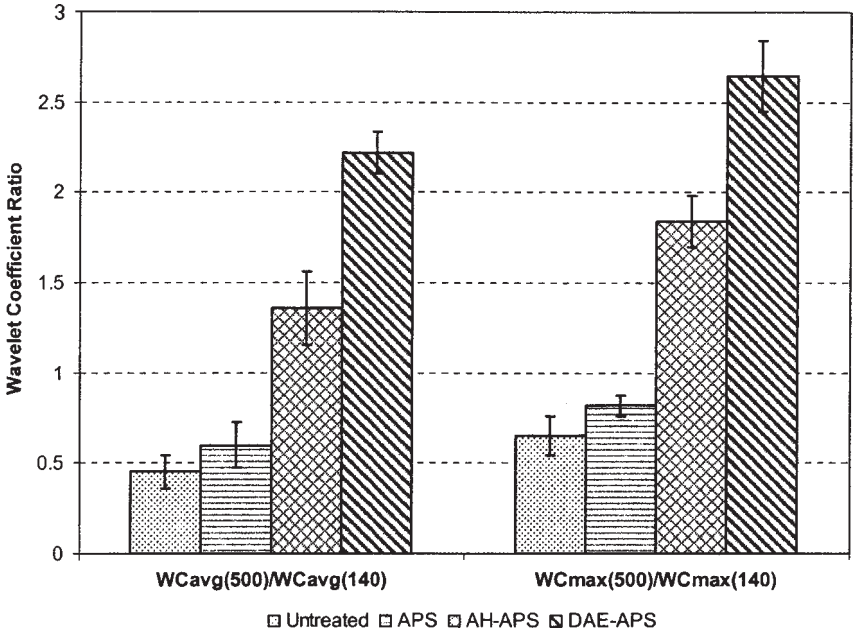

FIGURE 8 Comparison of WC ratios among various samples of glass beads treated with aminosilanes. Glass beads treated with APS show similar WC ratios leading to a strong contact adhesion mechanism just as the untreated beads do. From glass beads treated with APS to diaminosilane (AH-APS) to triaminosilane (DAE-APS), WC ratios increase. This suggests that the higher WC reveals a diffusion adhesion mechanism.

Downloaded At: 08:44 22 January 2011

and diffusion-adhesion mechanisms in the sense that the higher the WC ratios, the greater the penetration. It is noticed that the increase in WC ratios is proportional to the number of amino groups. This result would correlate well with an expectation that the increase in the silane's functional length and compatibility with the polymer might allow it to diffuse into the polymer more easily and react with the hydroxyl groups, yielding higher adhesion strength.

4. CONCLUSIONS

The use of AE techniques integrated with SPC mechanical–optical testing has been shown to be successful for characterizing adhesion in glass bead/PVB systems. It has been demonstrated that not only can an intrinsic interfacial strength be determined, but it may be speculated that different types of adhesion mechanisms may be

distinguished as well in terms of straightforward WC ratios from the wavelet transform WT of the acoustic debonding signals, once problems with edge reflections in the test coupon are resolved. The constraints for the WC ratio comparison to be meaningful are that not only must all the interrogated sources propagate in a plate with similar mechanical properties and thickness, but also that they are all released at a similar depth from the top surface, where a sensor is mounted. Ultimately, our study has shown that when the ambiguities inherent in AE testing of composite materials are clearly understood, the WT technique would give an AE practitioner a useful tool for the distinction of various failure sources of interest (*e.g.*, delamination, crazing, shear band formation, and cavitation) in a composite material specimen under stress.

ACKNOWLEDGMENTS

This work was supported by the Engineering Center for Surfaces, Polymers, and Colloids at the University of Washington. Helpful discussions with Dr. Marvin A. Hamstad, University of Denver, Department of Engineering, are also gratefully acknowledged.

Downloaded At: 08:44 22 January 2011

REFERENCES

[1] Moon, C. K. and McDonough, W. G., *J. Appl. Polym. Sci.* **67**, 1701–1709 (1998).
[2] Zhang, C. and Qiu, Y., *J. Adhes. Sci. Technol*. **17**, 397–408 (2003).
[3] Harding, P. H. and Berg, J. C., *J. Adhes. Sci. Technol*. **11**, 1063–1076 (1997).
[4] Miller, A. C. and Berg, J. C., *Composites: Part A* **34**, 327–332 (2003).
[5] Nguyen, F. N. and Berg, J. C., *J. Adhes. Sci. Technol*. **18**, 1011–1026 (2004).
[6] Scruby, C. B., *J. Phys. E: Sci. Instrum*. **20**, 946–953 (1987).
[7] Harding, P. H. and Berg, J. C., *J. Adhes. Sci. Technol*. **11**, 471–493 (1997).
[8] Plueddemann, E. P., *Silane Coupling Agents* (Plenum Press, New York, 1989), Chap. 3, pp. 49–75.
[9] Achenbach, J. D., *Wave Propagation in Elastic Solids* (North-Holland Publishing Company, New York, 1973), Chaps. 5–6, pp. 165–261.
[10] Hamstad, M. A., O'Gallacher, A., and Gary, J., *J. Acoustic Emission* **20**, 39–61 (2002).
[11] Gorman, M., *Nondestr. Test. Eval*. **14**, 89–104 (1998).
[12] Ostuka, H. and Scarton, H. A., *J. Composite Materials* **5**, 591–597 (1981).
[13] Valentin, D., Bonniau, P., and Bunsell, A. R., *Composites* **14**, 345–351 (1983).
[14] Favre, J. P. and Laizer, J. C., *Composites Sci. Tech*. **36**, 27–43 (1989).
[15] Guild, F. J., Phillips, M. G., and Harris, B., *NDT International* **Oct**., 209–218 (1980).
[16] Beattie, A. G., *Mat. Eval*. **34**, 73–78 (1976).
[17] Miller, A. C., Minko, S., and Berg, J. C., *J. Adhes*. **75**, 257–266 (2001).
[18] Minko, S., Karl, A., Voronov, A., Senkovskij, V., Pomper, Wilke, T. W., Malz, H., and Pionteck, J., *J. Adhes. Sci. Technol*. **14**, 999–1019 (2000).

[19] Cunis, S., Gehrke, R., Hartmann, K., Heise, B., Karl, A., Krosigk, G. V., Lode, U., Luzinov, I., Minko, S., Pomper, T., Voronov, A., and Wilke, W., *Eurofillers* **97**, 487–490 (1997).
[20] Karl, A., Cunis, S., Gehrke, R., Krosigk, G. V., Lode, U., Luzinov, I., Minko, S., Pomper, T., Senkovsky, V., Voronov, A., and Wilke, W., *J. Macromol. Sci. Phys*. **B38**, 901–912 (1999).
[21] Karl, A., Cunis, S., Gehrke, R., Krosigk, G. V., Lode, U., Luzinov, I., Minko, S., Pomper, T., Senkovsky, V., Voronov, A., and Wilke, W., *J. Macromol. Sci. Phys*. **B38**, 913–929 (1999).
[22] Ohta, M., Nakamura, Y., Hamada, H., and Maekawa, Z. I., *Polym. Polym. Composites* **2**, 215–221 (1994).
[23] Kraus, R., Wilke, W., Zhuk, A., Luzinov, I., Minko, S., and Voronov, A., *J. Mater. Sci*. **32**, 4397–4403 (1997).
[24] Kraus, R., Wilke, W., Zhuk, A., Luzinov, I., Minko, S., and Voronov, A., *J. Mater. Sci*. **32**, 4405–4410 (1997).
[25] Prosser, W. H., Jackson, K. E., Smith, B. T., McKeon, J., and Friedman, A., *Mater. Eval*. **53**, 1052–1058 (1995).
[26] Suzuki, H., Kinjo, T., and Takemoto, M., *J. Acoustic Emission* **14**, 69–84 (1996).
[27] Hamstad, M. A., O'Gallagher, A., and Gary, J., *J. Acoustic Emission* **19**, 258–274 (2001).
[28] Harding, P. H. and Berg, J. C., *J. Appl. Polym. Sci*. **67**, 1025–1033 (1998).

Downloaded At: 08:44 22 January 2011